Kodama S, Shu M, Saito K, Murakami H, Tanaka K, Kuno S, Ajisaka R, Sone Y, Onitake F, Takahashi A, Shimano H, Kondo K, Yamada N, Sone H.	Even low-intensity and low-volume exercise training may improve insulin resistance in the elderly.	Intern Med	46	1071-1077	2007
Kamijo K, Nishihira Y, Sakai T, Higashuura T, Kim SR, Tanaka K.	Effects of a 12-week walking program on cognitive function in older adults.	Advances in Exercise and Sports Physiology	13	31-39	2007
松尾知明, 室武由香子, 齋藤義浩, 大藏倫博, 中田由夫, 田中喜代次.	減量介入前の体格, 食事摂取量, 身体活動量が体重減少量に及ぼす影響.	肥満研究	13	154-163	2007
加藤祐介, 清野諭, 大河原一憲, 沼尾成晴, 新村由恵, 山吹啓介, 田中喜代次.	中高年男性における総合的体力および体力因子とメタボリックシンドロームとの関係.	肥満研究	13	283-289	2007
林容市, 鈴木宏哉, 沼尾成晴, 田中喜代次.	強度を自己選択した有酸素性運動中における生理的要因の経時変化と自覚的運動強度との相互関係.	体育学研究	52	119-131	2007
重松良祐, 中垣内真樹, 岩井浩一, 藪下典子, 新村由恵, 田中喜代次.	運動実践の頻度別にみた高齢者の特徴と運動継続に向けた課題.	体育学研究	52	173-186	2007
鰺坂隆一, 村上晴香, 前田清司, 久野譜也, 田中喜代次, 渡辺重行, 青沼和隆, 山口巌, 大槻毅, 家光素行, 曽根博仁.	中高齢者における高感度CRPと運動耐容能の関連および運動トレーニング効果.	心臓	39 (Suppl. 2)	12-14	2007
鰺坂隆一, 田辺匠, 村上晴香, 前田清司, 田中喜代次, 曽根博仁, 久野譜也, 大槻毅.	健常中高齢者における運動トレーニングの血清高感度CRP濃度に対する効果.	体力科学	56	179-190	2007
田中喜代次, 中田由夫, 大河原一憲, 片山靖富, 沼尾成晴, 松尾知明, 大藏倫博.	肥満研究に関する未解決の課題.	臨床運動療法研究会誌	9	36-42	2007

新村由恵, 田中喜代次, 坂井智明, 藪下典子.	筑波大学における要支援・特定高齢者向け運動プログラムー自宅で継続して実践できるー.	臨床運動療法研究会誌	9	30-33	2007
中田由夫, 大河原一憲, 片山靖富, 松尾知明, 沼尾成晴, 大藏倫博, 田中喜代次.	食事制限は運動実践を加えることによる効果は肥満度によって異なる：The SMART Study.	臨床運動療法研究会誌	9	54	2007
烏雲格日勒, 藤井勝紀, 花井忠征, 田中喜代次.	中国の蒙古族青少年の身長発育における時代的考証- 1985年と2005年との比較- .	教育医学	53	215-230	2007
柳久子, 奥野純子, 戸村成男, 大藏倫博, 田中喜代次.	軽度要介護者の血中ビタミンDレベルの分布状況とビタミンD・カルシウム製剤補充による介護予防効果- 生活機能・身体機能と血中ビタミンDレベルとの関連より- .	Osteoporosis Japan	15	677-681	2007
Son BK, Akishita M, Iijima K, Kozaki K, Maemura K, Eto M, Ouchi Y.	Adiponectin Antagonizes Stimulatory Effectof TNF{alpha} on Vascular Smooth Muscle Cell Calcification: Regulation of Gas6-Mediated Survival Pathway by AMP-Activated Protein Kinase.	Endocrinology			2008
Ota H, Akishita M, Eto M, Iijima K, Kaneki M, Ouchi Y.	Sirt1 modulates premature senescence-like phenotype in human endothelial cells.	J Mol Cell Cardiol.	43	571-9.	2007
Teramoto S, Yamaguchi Y, Yamamoto H, Hanaoka Y, Ishii M, Hibi S, Kume H, **Akishita M**, Ouchi Y.	Effects of age and sex on plasma adrenomedullin levels in patients with obstructive sleep apnea syndrome.	J Am Geriatr Soc.	55	1891-2	2007
Akishita M, Hashimoto M, Ohike Y, Ogawa S, Iijima K, Eto M, Ouchi Y.	Association of plasmadehydroepiandrosterone-sulfate levels with endothelial function in postmenopausal women with coronary risk factors.	Hypertens Res.			in press

Akishita M, Hashimoto M, Ohike Y, Ogawa S, Iijima K, Eto M, Ouchi Y.	Low testosterone level is an independent determinant of endothelial dysfunction in men.	Hypertens Res.	30	1029-1034	2007
Xi H, **Akishita M**, Nagai K, Yu W, Hasegawa H, Eto M, Kozaki K, Toba K.	Potent free radical scavenger, edaravone, suppresses oxidative stress-induced endothelial damage and early atherosclerosis.	Atherosclerosis.	191	281-289	2007
Yu J, Eto M, **Akishita M**, Kaneko A, Ouchi Y, Okabe T.	Signaling pathway of nitric oxide production induced by ginsenoside Rb1 in human aortic endothelial cells: A possible involvement of androgen receptor.	Biochem Biophys Res Commun.	353	764-9	2007
Son BK, Kozaki K, Iijima K, Eto M, Nakano T, **Akishita M**, Ouchi Y.	Gas6/Axl-PI3K/Akt pathway plays a central role in the effect ofstatins on inorganic phosphate-induced calcification of vascular smooth muscle cells	Eur J Pharmacol.	556	1-8	2007
Okauchi Y, Nishizawa H, Funahashi T, Ogawa T, Noguchi M, Ryo M, Kihara S, Iwahashi H, Yamagata K, Nakamura T, Shimomura I, Matsuzawa Y.	Reduction of visceral fat is associated with decrease in the number of metabolic risk factors in Japanese men	Diabetes Care	30	2392-2394	2007
Saito Y, Yamada N, Shirai K, Sasaki J, Ebihara Y, Yanase T, Fox JC.	Effect of rosuvastatin 5-20mg on triglycerides and other lipid parameters in Japanese patients with hypertriglycerides.	Atherosclerosis	194(2)	505-11	2007

Oikawa S, Kita T, Sasaki J, et al.	Risk of coronary events in Japanese patients with both hypercholesterolemia and type2 diabetes mellitus on low-dose simvastatin therapy: Implication from Japan Lipid Intervention Trial(J-LIT).	Atherosclerosis	191(2)	440-6	2007
Matsuzawa Y, Kita T, Shepherd J, Gotto AM Jr, Nakamura H, Sacks FM, Oikawa S, Sasaki J	A triology of primary prevention statin trials.	Atherosclerosis	Suppl 8(2)	19-24	2007
Okamura T, Nakamura K, Kanda H, Hayakawa T, Hozawa A, Murakami Y, Kadowaki T, Kita Y, Okayama A, Ueshima H; Health Promotion Research Committee, Shiga National Health Insurance Organizations	Effect of combined cardiovascular risk factors on individual and population medical expenditures: a 10-year cohort study of national health insurance in a Japanese population	Circ J	71(6)	807-13	2007
Kadota A, Hozawa A, Okamura T, Kadowak T, Nakmaura K, Murakami Y, Hayakawa T, Kita Y, Okayama A, Nakamura Y, Kashiwagi A, Ueshima, H NIPPON DATA Research Group	Relationship between metabolic risk factor clustering and cardiovascular mortality stratified by high blood glucose and obesity: NIPPON DATA90, 1990-2000	Diabetes Care	30(6)	1533-8	2007
Nakamura Y, Turin TC, Kita Y, Tamaki S, Tsujita Y, Kadowaki T, Murakami Y, Okamura T, Ueshima H	Associations of obesity measures with metabolic risk factors in a community-based population in Japan	Circ J	71(5)	776-81	2007

T Takayama, T Hiro, M Yamagishi, H Daida, S Saito, T Yamaguchi, M Matsuzaki	Rationale and Design for a Study Using Intravascular Ultrasound to Evaluate Effects of Rosuvastatin on Coronary Artery Atheroma in Japanese Subjects: COSMOS Study(Coronary Atherosclerosis Study Measuring Effects of Rsuvastatin Using Intravascular Ultrasound in Japanese Subjects)	Circ J	71(2)	271-275	2007
K Shimamoto, T Kita, H Mabuchi, M Matsuzaki, Y Matsuzawa, N Nakaya, S Oikawa, Y Saito, J Sasaki, H Itakura, the J-LIT Study Group	Effects of Hypertension and Type 2 Diabetes Mellitus on the Risk of Total Cardiovascular Events in Japanese Patients with Hypercholesterolemia : Implications from the Japan Lipid Intervention Trial(J-LIT)	Hypertens Res	30(2)	119-123	2007
M Yokoyama, H Origasa, M Matsuzaki, Y Matsuzawa, Y Saito, Y Ishikawa, S Oikawa, J Sasaki, H Hishida, H Itakura, T Kita, A Kitabatake, N Nakaya, T Sakata, K Shimada, K Shirato, for the Japan EPA lipid intervention study (JELIS) Investigators	Effects of eicosapentaenoic acid on major coronary events in hypercholesterolaemic patients (JELIS): a randomised openlabel, blinded endpoint analysis	Lancet	369	1090-1098	2007

S Oikawa, T Kita, H Mabuchi, M Matsuzaki, Y Matsuzawa, N Nakaya, Y Saito, J Sasaki, K Shimamoto, H Itakura, The J-LIT Study Group	Risk of coronary events in Japanese patients with both hypercholesterolemia and type 2 diabetes mellitus on low-dose simvastatin therapy: Implication from Japan Lipid Intervention Trial (J-LIT)	Atherosclerosis	191	440-446	2007
A Takaki, H Ogawa, T Wakeyama, T Iwami, M Kimura, Y Hadano, S Matsuda , Y Miyazaki, T Matsuda, A Hiratsuka, M Matsuzaki	Cardio-Ankle Vascular Index is a New Noninvasive Parameter of Arterial Stiffness	Circ J	71(11)	1710-1714	2007
H Aoki, K Yoshimura, M Matsuzaki	Turning back the clock: regression of abdominal aortic aneurysms via pharmacotherapy	J Mol Med	85(10)	1077-1088	2007
Y Fukumoto, T Hiro、T Fujii, G Hashimoto, J Yamada, T Okamura, T Fujimura, M Matsuzaki	Localized Elevation of Shear Stress is Related to Coronary Plaque Rupture: A Three-dimensional Intravascular Ultrasound Study with In Vivo Color Mapping of Shear Stress Distribution	J Am Coll Cardiol	51(6)	654-650	2008
A Matsushima, H Nakamura, S Umemoto, M Matsuzaki	Regulation of Cardiac Regeneration by ACE Inhibition Following Donor Heart Myocardial Infarction after Heterotopic Transplantation in Tg mice	Circ J			in press
吉金秀樹, 山本健, 尾崎正治, 松﨑益徳	生活習慣病, メタボリックシンドロームにおける高感度C反応性蛋白の臨床的意義	J Cardiol	50(3)	175-182	2007
Ueda A, Kume N, Hayashida K, Inui-Hayashida A, Asai M, Kita T, Kominami G	ELISA for soluble form of lectin-like oxidized LDL receptor-1, a novel marker of acute coronary syndrome.	Clin. Chem.	Vol. 52	1210-1211	2006

Aramaki Y, Mitsuoka H, Toyohara M, Jinnai T, Kanatani K, Nakajima K, Mukai E, Yamada Y, Kita T, Inagaki N, Kume N	Lectin-like oxidized LDL receptor-1 (LOX-1) acts as a receptor for remnant-like lipoprotein particles (RLPs) and mediated RLP-induced migration of vascular smooth muscle cells.	Atherosclerosis	印刷中	印刷中	2008
Iwai-Kanai E., Ogawa F., Nakagawa M., Nishimura T., Matsubara H., Naruse S.	The Role of Group Brain Check-up Using Magnetic Resonance Imaging in pre-Elderly with Hypertension.	***Progress in C. I.***	28(1)	28(1)	2006
Aramaki Y, Mitsuoka H, Toyohara M, Jinnai T, Kanatani K, Nakajima K, Mukai E, Yamada Y, Kita T, Inagaki N, and Kume N.	Lectin-like LDL receptor-1 (LOX-1) acts as a receptor for remnant-like lipoprotein particles (PLPs) and mediates RLP-induced migration of vascular smooth muscle cells.	Atherosclerosis			in press. (2008)
Fujiwara H, Hosokawa M, Zhou X, Fujimoto S, Fukuda K, Toyoda K, Nishi Y, Fujita Y, Yamada K, Yamada Y, Seino Y, and Inagaki N.	Curcumin inhibits glucose production in isolated mice hepatocytes.	Diabetes Res. Clin. Pract			in press (2008)
Yamada C, Yamada Y, Tsukiyama K, Yamada K, Udagawa N, Takahashi N, Tanaka K, Drucker DJ, Seino Y, and Inagaki N.	The murine Glp1r is essential for control of bone resorption.	Endocrinology	149	574-579	2008
Toyoda K, Okitsu T, Yamane S, Uonaga T, Liu X, Harada N, Uemoto S, Seino Y, and Inagaki N.	GLP-1 receptor signaling protects pancreatic beta cells in intraportal islet transplant by inhibiting apoptosis.	Biochem. Biophys. Res. Commun	367(4)	793-798	2008

Toyoda K, Fukushima M, Mitsui R, Harada N, Suzuki H, Takeda T, Taniguchi A, Nakai, Y Kawakita T, Yamada Y, Inagaki N, Seino Y.	Factors responsible for age-related elevation in fasting plasma glucose: a cross-sectional study in Japanese Men.	Metabolism	57(2)	299-303	2008
Harada N, Yamada Y, Tsukiyama K, Yamada C, Nakamura Y, Mukai E, Hamasaki A, Liu X, Toyoda K, Seino Y, and Inagaki N	A novel gastric inhibitory polypeptide (GIP) receptor splice variant influences GIP sensitivity of pancreatic β-cells in obese mice.	Am. J. Physiol. Endocrinol. Metab.	294(1)	E61-68	2008
Yamada C, Yamada Y, Tsukiyama K, Yamada K, Yamane S, Harada N, Miyawaki K, Seino Y, and Inagaki N.	Genetic inactivation of GIP signaling reverses aging-associated insulin resistance through body composition changes.	Biochem. Biophys. Res. Commun.	364	175-180.	2007
Taniguchi A, Fukushima M, Kuroe A, Sakaguchi K, Hashimoto H, Yoshioka I, Kitatani N, Tsuji T, Ohya M, Ohgushi M, Nagasaka S, Isogai O, Nakai Y, Inagaki N, and Seino Y.	Metabolic syndrome, insulin resistance, and atherosclerosis in Japanese type 2 diabetic patients..	Metabolism	56	1099-1103	2007
Ohgushi M, Taniguchi A, Fukushima M, Nakai Y, Kuroe A, Ohya M, Nagasaka S, Taki Y, Yoshii S, Matsumoto K, Yamada Y, Inagaki N, and Seino Y.	Soluble tumor necrosis factor receptor 2 is independently associated with pulse wave velocity in nonobese Japanese patients with type 2 diabetes mellitus.	Metabolism	56	571-577	2007

Numaoa S, Hayashi Y, Katayama Y, Matsuo T, Tomita T, Ohkawara K, Nakata Y, Okura T, Tanaka K	Plasma fat concentration increases in visceral fat obese men during high-intensity endurance exercise	Obesity Research & Clinical Practice	1	273-279	2007
Okura T, Nakata Y, Ohkawara K, Numao S, Katayama Y, Matsuo T, Tanaka K	Effect of aerobic exercise on metabolic syndrome improvement in response to weight reduction	Obesity	15	2478-2484	2007
松尾知明, 室武由香子, 齋藤義浩, 大藏倫博, 中田由夫, 田中喜代次	減量介入前の体格, 食事摂取量, 身体活動量が体重減少量に及ぼす影響	肥満研究	13	154-163	2007
Okura T, Nakata Y, Ohkawara K, Numao S, Katayama Y, Ono Y, Matsuo T. Tanaka K	Effects of weight reduction on concentration of plasma total homocysteine in obese Japanese men	Obesity Research & Clinical Practice	1	213-221	2007
Matsuo T, Okura T, Nakata Y, Yabushita N, Numao S, Sasai H, Tanaka K	The influence of physical activity-induced energy expenditure on the variance in body weight change among individuals during a diet intervention	Obesity Research & Clinical Practice	1	109-117	2007
柳 久子、奥野純子、戸村成男、大藏倫博、田中喜代次	軽度要介護者の血中ビタミンDレベルの分布状況とビタミンD・カルシウム製剤補充による介護予防効果－生活機能・身体機能と血中ビタミンDレベルとの関連より－	Osteoporosis Japan	15	677-681	2007

Ⅳ. 研究成果の刊行物・別冊

Available online at www.sciencedirect.com
ScienceDirect
ELSEVIER
Biochemical and Biophysical Research Communications 353 (2007) 764–769
BBRC
www.elsevier.com/locate/ybbrc

Signaling pathway of nitric oxide production induced by ginsenoside Rb1 in human aortic endothelial cells: A possible involvement of androgen receptor

Jing Yu [a], Masato Eto [b], Masahiro Akishita [b], Akiyo Kaneko [a], Yasuyoshi Ouchi [b], Tetsuro Okabe [a,*]

[a] *Department of Integrated Traditional Medicine, University of Tokyo Graduate School of Medicine, Tokyo, Japan*
[b] *Department of Gerontology, University of Tokyo Graduate School of Medicine, Tokyo, Japan*

Received 7 December 2006
Available online 22 December 2006

Abstract

Ginsenosides have been shown to stimulate nitric oxide (NO) production in aortic endothelial cells. However, the signaling pathways involved have not been well studied in human aortic endothelial cells. The present study was designed to examine whether purified ginsenoside Rb1, a major active component of ginseng could actually induce NO production and to clarify the signaling pathway in human aortic endothelial cells. NO production was rapidly increased by Rb1. The rapid increase in NO production was abrogated by treatment with nitric oxide synthetase inhibitor, L-NAME. Rb1 stimulated rapid phosphorylation of Akt (Ser473), ERK1/2 (Thr202/Thr204) and eNOS (Ser1177). Rapid phosphorylation of eNOS (Ser1177) was prevented by SH-5, an Akt inhibitor or wortmannin, PI3-kinase inhibitor and partially attenuated by PD98059, an upstream inhibitor for ERK1/2. Interestingly, NO production and eNOS phosphorylation at Ser1177 by Rb1 were abolished by androgen receptor antagonist, nilutamide. The results suggest that PI3kinase/Akt and MEK/ERK pathways and androgen receptor are involved in the regulation of acute eNOS activation by Rb1 in human aortic endothelial cells.

Keywords: Ginsenoside Rb1; Endothelial cells; Nitric oxide; eNOS; Androgen receptor; PI3-kinase; Akt; ERK; MEK; Phosphorylation

Ginseng, the root of Panax ginseng C.A. Meyer (Araliaceae), is a well-known and popular herbal medicine used worldwide. Among more than 30 ginsenosides, the active ingredient of ginseng, ginsenoside Rb1 is regarded as the main compound responsible for many pharmaceutical actions of ginseng. The oral administration of ginseng caused a decrease in blood pressure in essential hypertension [1]. Intravenous administration of ginsenosides (a mixture of saponin from Panax ginseng C.A. Meyer) lowered blood pressure in a dose-dependent manner in anesthetized rats [2]. Although these reports suggest that ginsenosides could stimulate the production of nitric oxide (NO) by aortic vascular endothelial cells, the precise mechanisms of the ginsenoside actions have not been fully elucidated [3]. NO released from endothelial cells via the endothelial nitric oxide synthetase (eNOS) is a pivotal vasoprotective molecule. In addition to its vasodilating feature, endothelial NO has anti-atherosclerotic properties, such as inhibition of platelet aggregation, leukocyte adhesion, smooth muscle cell proliferation, and expression of genes involved in atherosclerosis [4].

The present study aims at investigating the signaling pathways involved in NO production by purified ginsenoside Rb1 in human aortic endothelial cells in vitro.

Materials and methods

Materials. Rb1, nilutamide, L-NAME (hydrochloride), Hanks' balanced salt solution (HBSS) were purchased from Sigma (St. Louis, MO,

* Corresponding author. Fax: +813 5684 3987.
E-mail address: okabe-tky@umin.ac.jp (T. Okabe).

0006-291X/$ - see front matter © 2006 Elsevier Inc. All rights reserved.
doi:10.1016/j.bbrc.2006.12.119

USA). ICI182780 was from Zeneca Pharmaceuticals (Macdesfield, UK). 4,5-diaminofluorescin diacetate (DAF-2 DA) was purchased from Daiichi (Daiichi Pure Chemicals Co., Ltd, Tokyo, Japan). PD98059, SH-5, wortmannin and Nitric Oxide Synthase Assay Kit were from Calbiochem (EDM Biosciences, Inc., La Jolla, CA, USA and Germany). L-[^{3}H]Arginine was purchased from Amersham (Amersham Biosciences, Uppsala, Sweden). Antibody of phospho-eNOS (Ser1177) was from upstate (Upstate Inc., Lake Placid, NY). Antibody for eNOS/NOS type III was purchased form BD Transduction Laboratories (BD Biosciences, Franklin Lakes, NJ, USA). All other antibodies were form Cell Signaling Technology (Beverly, MA, USA). LumiGLO Reserve Chemiluminescent Substrate Kit was from KPL (Gaithersburg, MD, USA). EBM-2 (endothelial cell base medium) was from Clonetics (Walkersville, MD, USA). Human aortic endothelial cells (HAECs) were from Cambrex (Cambrex BioScience Walkersville, Inc. Walkersville, MD, USA). Fetal bovine serum (FBS) was from CCT (Sanko Junyaku Co., Ltd, Tokyo, Japan), Fetal bovine serum charcoal stripped was from MultiSer (ThermoTrace Ltd., Melbourne, Australia).

Cell culture. HAECs were cultured in a 37 °C humidified atmosphere of 95% air/5% CO_2 in EGM-2 (endothelial cell grows medium 2) medium supplemented with 10% FBS. The EGM-2 medium consisted of 0.1% EGF, 0.04% hydrocortisone, 0.4% hFGF-B, 0.1% VEGF, 0.1% R^3-IGF-1, 0.1% ascorbic acid, 0.1% GA-1000, and 0.1% heparin. Experiments were performed with cells from passages 5 to 7. For all experiments, HAECs were plated at a concentration of 1×10^4/mL and grown to confluence. Then cells were serum-starved for 6 h in phenol red free EBM-2 containing 1% DCC-FBS, that was removed the steroid by processing it with dextran-coated charcoal (DCC-FBS). In some inhibitory experiments, the inhibitors were added to cells 60 min before the stimuli. DMSO was used as a solvent for Rb1, PD98059, wortmannin, SH-5, L-NAME, nilutamide, and DAF-2 DA present at equal concentrations (0.01%) in all groups, including the vehicle.

Western blot analysis. After treatment with reagents, confluent monolayers of cells were washed two times in ice-cold phosphate-buffered saline and lysed with buffer containing 20 mmol/L Tris–HCl (pH 7.5), 150 mmol/L NaCl, 1 mmol/L EDTA, 1 mmol/L EGTA, 1% Triton-X, 2.5 mmol/L sodium pyrophosphate, 1 mmol/L β-glycerophosphate, 1 mmol/LNa_3VO_4, 1 μg/mL Leupeptin, 1 mM PMSF). For western blot analysis, total cell lysate was subjected to SDS-polyacrylamide gel electrophoresis (PAGE), and proteins were transferred to poly vinilidene difluoride (PVDF) membrane. The antibodies used in this study were anti-phospho-ERK1/2 (Thr202/Thr204), anti-ERK1/2, anti phospho-Akt (Ser473), anti-Akt, anti-phosph-eNOS (ser1177) and anti-NOS. Antibodies were detected by means of a horseradish peroxidase-linked secondary antibody and immunoreactive bands were visualized using LumiGLO Reserve Chemiluminescent Substrate Kit.

Endothelial NO synthase activity assay. Endothelial cell NO synthase (eNOS) activity was quantified by measuring the conversion of L-[^{3}H]-arginine to L-[^{3}H]-citrulline by the use of a NO synthase assay kit.

Measurement of intracellular production of NO. Production of NO was assessed using the NO-sensitive fluorescent dye DAF-2 DA [5]. Briefly, confluent cells were serum-staved for 6 h. Because NOS generates O_2^- instead of NO in the absence of L-arginine, so L-arginine (100 μmol/L) was add 1 h prior to all solutions, except for the experiment with *N*-nitro-L-arginine methyl ester (L-NAME; a NOS inhibitor)-treated cells. Cells were loaded with DAF-2 DA (final concentration 5 μmol/L, 30 min 37 °C) and than rinsed three times with HBSS, kept in the dark, and maintained at 37 °C in 1% EBM-2 medium with a warming stage. After 30 min, cells were then treated with Rb1 or other stimuli. In some inhibitory experiments, the inhibitors were administered 30 min before loading with DAF-2 DA. Green fluorescence intensity was measured with a laser scanning confocal microscopy system (LSCM) (Bio-Rad Laser Sharp2000). The fluorescence image was obtained as a 512 × 512 pixel frame. Ex = 488 nm, EM = 510 nm. All other settings, including scanning speed, pinhole diameter, and voltage gain, remained the same for all experiments.

Statistics. Data are means ± SEM. Statistical comparisons were performed by Student's *T* test between two groups. A value of $P < 0.05$ was considered significant.

Results

Rb1 stimulates rapid production of NO in human aortic endothelia cells

We used the NO-specific fluorescent dye DAF-2 DA to evaluate the effect of Rb1 on NO production in HAECs. 5, 10, 15, 30, 60, 120 and 180 min after Rb1 treatment, cells were fixed and then viewed using a fluorescence microscope. Emission of green light (510 nm) from cells excited by light at 488 nm is indicative of NO production. A significant increase in green fluorescence was observed >15 min after the addition of Rb1 and lasted for 60 min in HAECs (Fig. 1A). Maximal stimulation of NO production was obtained at 30 min.

To verify that the rapid increase in green fluorescence in response to Rb1 treatment specifically reflected NO production, we compared results from HAECs treated with acetylcholine (1 μmol/L) or Rb1 (1 μmol/L) for 5 min. Reassuringly, treatment with either acetylcholine and calcium ionophore or Rb1 resulted in a increase in green fluorescence (Fig. 1B). We next examined the effects of the NOS inhibitor L-NAME to determine whether the NO increase was attributable to NOS derived de novo synthesis. As shown in Fig. 1C, the Rb1-induced DAF-2 DA fluorescence was completely suppressed by pretreatment with L-NAME (0.5 mmol/L). The results suggested that the rapid increase in NO production after Rb1 treatment was mediated by an increase in NOS activity.

Rb1 stimulates phosphorylation of eNOS (Ser1177) and increases NOS activity

To examine involvement of eNOS in the NO increase, the effect of Rb1 on eNOS phosphorylation at Ser-1177 was tested by Western blotting. As shown in Fig. 2, Rb1 induced rapid eNOS phosphorylation after 10 min of incubation, maximal eNOS phosphorylation by Rb1 was observed from 30 to 60 min of incubation. The relative magnitude of eNOS phosphorylation falls subsequently but is still significantly greater than control after 120 min of Rb1 incubation (Fig. 2A, upper blots). The acute effect by Rb1 on eNOS phosphorylation was concentration dependent (Fig. 2B, upper blots). Rb1 did not affect eNOS protein expression (Fig. 2A and B, lower blots).

To see whether Rb1 actually activates NOS in HAECs, we measured NOS activity after 30 min of treatment with Rb1. As shown in Fig. 2C, Rb1 significantly increased NOS activity in HAECs.

PI3-kinase/Akt and MEK/ERK pathways are involved in eNOS phosphorylation and NO production

Previous studies have demonstrated that PI3-kinase/Akt and MEK/ERK pathways are two important signaling cascades mediating eNOS activation by many stimuli in vascular endothelial cells [6,7]. Therefore, we examined

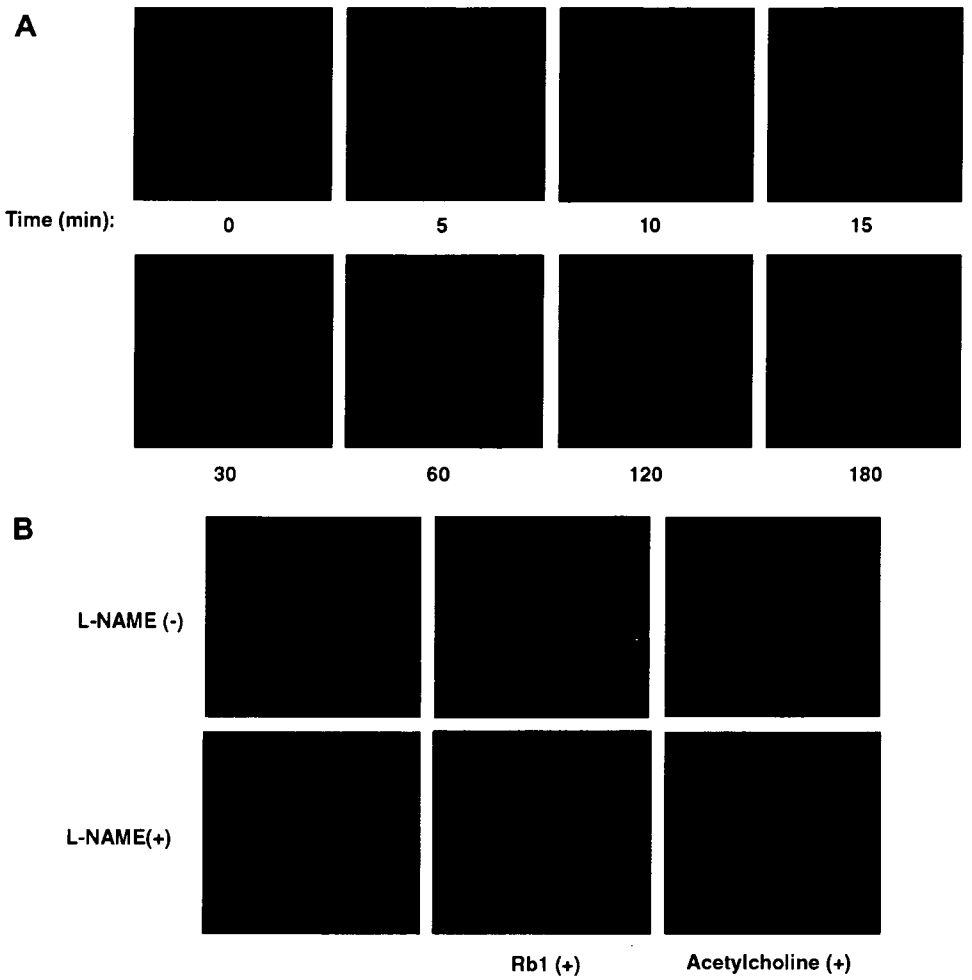

Fig. 1. Effect of Rb1 on production of NO. HAECs were starved and loaded with DAF-2 DA (5 μmol/L) as described in Materials and methods prior to treatment with either Rb1 (1 μmol/L) for 0, 5, 10, 15, 30, 60, 120, and 180 min (A) or acetylcholine (1 μmol/L) for 5 min (B). After Rb1 treatment, cells were fixed in 2% paraformaldehyde for 10 min at 4 °C and then viewed using a fluorescent microscope. Emission of green light (510 nm) from cells excited by light at 488 nm is indicative of NO production. In some groups of cells, L-NAME (0.5 mmol/L) was added 30 min before loading cells with DAF-2 DA (B). A representative time course experiment is shown for experiments that were repeated independently for three times. (For interpretation of the references to color in this figure legend, the reader is referred to the web version of this paper.)

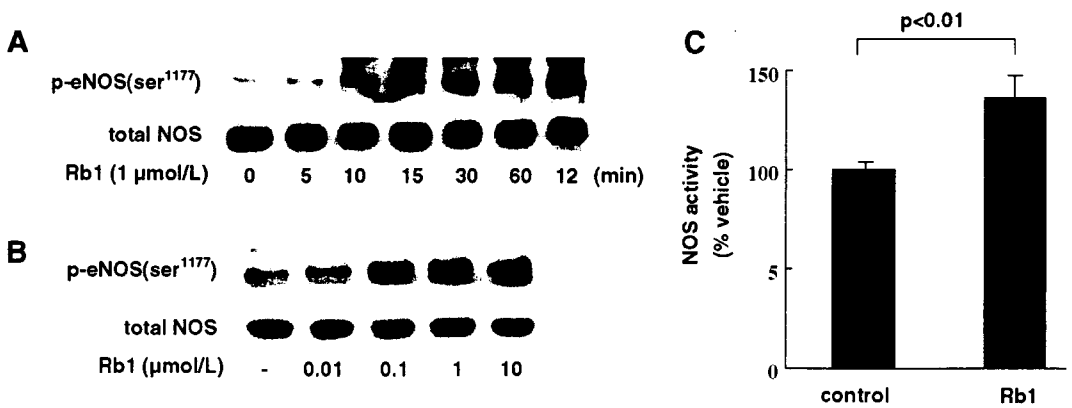

Fig. 2. Effects of Rb1 on eNOS phosphorylation and NOS activity. Phosphorylation of eNOS in HAECs. Starved HAECs were treated with the vehicle (0.01% DMSO) or Rb1 (1 μmol/L) for indicated times (A) or with various concentrations of Rb1 for 30 min (B). Western analysis performed to detect phospho-eNOS (Ser1177) and total eNOS. The experiments were repeated three times in triplicates, with equal result. NOS activity in HAECs homogenates. Rb1 (1 μmol/L) were added to the starved medium for 30 min, then activity of NOS was measured by the conversion of L-arginine to L-citrulline at 37 °C for 60 min (C). Histograms and error bars represent means ± SEM of four independent experiments performed in duplicate. $^{*}P < 0.01$ vs control.

whether Rb1 activated Akt and ERK1/2. We used phospho-specific antibodies to evaluate the ability of Rb1 to stimulate phosphorylation of Akt and ERK1/2 in HAECs. Rb1 rapidly increased phosphorylation of Akt (Ser473) and ERK1/2 (Fig. 3A, upper blots) in HAECs > 5 min after the addition of Rb1. Maximal phosphorylation was attained at 30 min in Akt and at 15 min in ERK1/2. The relative magnitude of the Rb1 response falls subsequently but is still significantly greater than control after 120 min of Rb1 treatment. Rb1 did not affect total Akt and ERK protein expression (Fig. 3A, lower blots).

We next examined the rapid phosphorylation of eNOS at Ser1179 by Rb1 either in the absence or presence of PI3 kinase inhibitor wortmannin, and Akt inhibitor SH-5 or MEK (ERK kinase) inhibitor PD98059. As shown in Fig. 3B, the rapid eNOS phosphorylation was abolished by pretreatment of cells with wortmannin (5 μmol/L) or SH-5, and partially attenuated by MEK inhibitor PD98059 (10 μmol/L). NO production viewed by fluorescent microscopy showed the similar inhibition by these inhibitors (Fig. 3C). These results suggest that acute activation of eNOS and NO production by Rb1 were mediated through activation of PI3-kinase/Akt and ERK1/2.

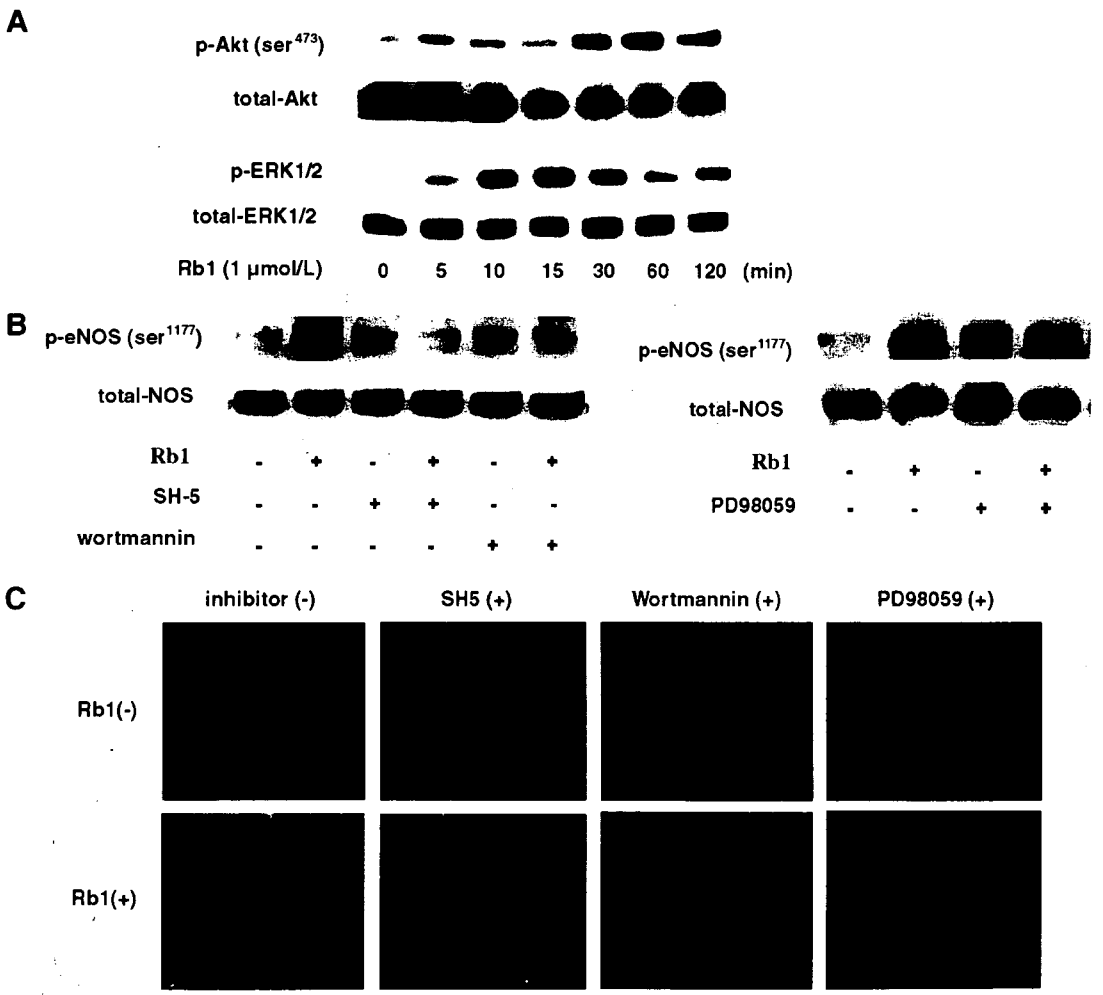

Fig. 3. Effects of inhibitors for PI3kinae/Akt or MEK (ERK kinase) on eNOS phosphorylation and NO production. Starved HAECs were treated with the vehicle (0.01% DMSO) or Rb1 (1 μmol/L) for indicated times (A). In some groups, cells were pretreated with SH-5 (10 μmol/L), wortmannin (5 μmol/L) or PD98059 (10 μmol/L) for 1 h, then cells were treated without or with Rb1 (1 μmol/L) for 30 min (B). Cell lysates were analyzed by Western blot as described in Materials and methods. Anti-phospho-Akt (Ser473) antibody and anti-Akt antibody; anti-phospho-ERK1/2 antibody and anti-ERK1/2 antibody (A), anti-phospho-eNOS (Ser1177) antibody and anti-eNOS antibody (B) were used for western blot analysis. Experiments were repeated three times, with equivalent result. Starved cells were loaded with DAF-2 DA as described in Materials and methods before treatment with Rb1 (1 μmol/L). In some groups of cells, SH-5 (10 μmol/L), wortmannin (5 μmol/L) or PD98059 (10 μmol/L) were added 60 min before cells were loaded with DAF-2 DA. After Rb1 treatment, cells were fixed in 2% paraformaldehyde for 10 min at 4 °C and then viewed using a fluorescent microscope (C). Emission of green light (510 nm) from cells excited by light at 488 nm is indicative of NO production. A representative set of experiments is shown for experiments that were repeated independently three times. (For interpretation of the references to color in this figure legend, the reader is referred to the web version of this paper.)

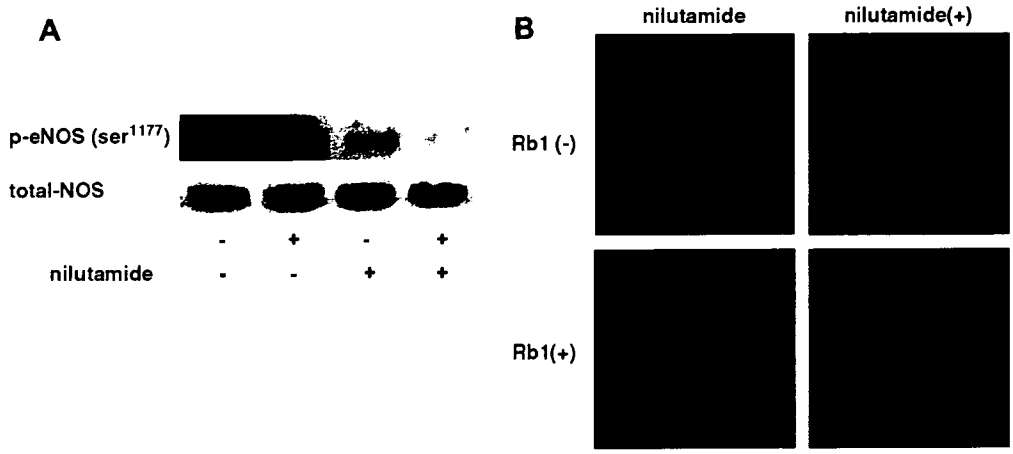

Fig. 4. Effects of nilutamide, an antagonist of androgen receptor, on eNOS phosphorylation and NO production. HAECs were starved 6 h and then treated without or with Rb1 (1 μmol/L) for 30 min. Some groups of cells were pre-treated with androgen receptor agonist nilutamide (10 μmol/L) for 1 h. Cell lysates were then subjected to immunoblotting as described in Materials and methods. The experiments were repeated three times in triplicates, with equal results. Starved cells were loaded with DAF-2 DA as described in Materials and methods before treatment with Rb1 (1 μmol/L). In some groups of cells, nilutamide (10 μmol/L) were added 60 min before cells were loaded with DAF-2 DA. After Rb1 treatment, cells were fixed in 2% paraformaldehyde for 10 min at 4 °C and then viewed using a fluorescent microscope (B). Emission of green light (510 nm) from cells excited by light at 488 nm is indicative of NO production. The experiments were repeated independently three times with equal results. (For interpretation of the references to color in this figure legend, the reader is referred to the web version of this paper.)

Rb1-induced eNOS phosphorylation is inhibited by androgen receptor antagonist

Increasing evidence shows that activation of the steroid hormone receptor such as estrogen receptor (ER) lead to NO production and vasodilation within minutes by non-transcriptional pathways. Ginsenosides have steroidal skeleton structure and can act as an agonist for steroid hormones receptor. To see whether steroid hormone receptors were involved in acute activation of eNOS to produce NO in HUACs by Rb1, we examined the effects of the androgen receptor antagonist nilutamide and estrogen receptor antagonist ICI182780. Representative western blots obtained using anti-phospho-eNOS (Ser1177) antibody and anti-eNOS antibody are shown in Fig. 4A. The Rb1-induced eNOS phosphorylation (Ser1177) was inhibited by the androgen receptor antagonist nilutamid (10 μmol/L) In addition, NO production was diminished to the baseline level in the presence of nilutamid (Fig. 4B). However, the Rb1-induced eNOS phosphorylation (Ser1177) and NO production were unaffected by an estrogen receptor (ER) antagonist ICI182780 (10 μmol/L) (data not shown).

Discussion

We have shown that purified Rb1 rapidly stimulates production of NO in HAECs > 15 min after treatment. Maximal stimulation of NO production was obtained at 30 min. The increase in NO production was abrogated by the addition of eNOS inhibitor, L-NAME. It is generally well known that eNOS is tightly regulated not only at the transcriptional level but also by several post-transcriptional mechanisms [8]. The enhanced phosphorylation at Ser1177 leads to increased eNOS activity. In our experiments, Rb1 induced rapid phosphorylation of eNOS at Ser1177 > 10 min after Rb1 treatment. Maximal eNOS phosphorylation by Rb1 was observed from 30 to 60 min of incubation. NOS activity was also increased by the addition of Rb1 in HAECs. Taken together, our results suggest that the acute effect on NO production in HAECs is attributable to rapid phosphorylation of eNOS at Ser1177. NO produced by eNOS is a fundamental determinant of cardiovascular homeostasis responsible for regulating systolic blood pressure, vascular remodeling and angiogenesis. It is possible to consider that Rb1, a major active component of ginseng could be a candidate responsible for the antihypertensive effects of ginseng previously reported [1,2].

Recent studies have revealed that PI3-kinase/Akt and MEK/ERK1/2 pathways are crucial regulator in cell proliferation, cell-cycle progression, and mediator of cellular survival. Both of them also contribute to enhanced phosphorylation of eNOS at Ser1177/1179 and production of NO [6,7]. The present study showed that Rb1 also stimulated the phosphorylation of Akt (Ser473) and ERK1/2 (Thr202/Thr204) in HAECs. Rb1-induced eNOS phosphorylation was prevented by inhibitors for PI3-kinase/Akt or MEK (ERK kinase). Our data suggest that the activation of PI3-kinase/Akt and MEK/ERK-mediated pathways are involved in the regulation of acute eNOS phosphorylation by ginsenoside Rb1 in HAECs.

Another interesting finding is that acute phosphorylation of eNOS by Rb1 was abolished by an antagonist for androgen receptor. Recent studies have shown Rb1 acts as a phytoestrogen in MCF-7 human mammary carcinoma

cells [9]. However, in HAECs, Rb1-induced eNOS phosphorylation was not prevented by an antagonist for estrogen receptor (data not shown). It is known that testosterone prevents coronary artery disease, and lower testosterone level is a risk factor for ischemic heart disease in men [10 12]. Recent studies revealed that endothelial NO has antiatherosclerotic properties, such as inhibition of platelet aggregation, leukocyte adhesion, smooth muscle cell proliferation, and expression of genes involved in atherosclerosis [4]. Together with these observations, our results that Rb1 induced eNOS phosphorylation has been abolished by the androgen receptor antagonist will be the beginning of the experimental analyses at cellular levels and may provide a clue for better understanding of the mechanisms by which androgens exert their action for preventing coronary artery disease. Further studies are required for elucidation.

Acknowledgments

We thank Drs. K. Yamamoto, K. Hasegawa, Y. Iwaoka, and S. Takasugi for their helpful advices and continuous encouragement.

References

[1] K.H. Han, S.C. Choe, H.S. Kim, D.W. Sohn, K.Y. Nam, B.H. Oh, M.M. Lee, Y.B. Park, Y.S. Choi, J.D. Seo, Y.W. Lee, Effect of red ginseng on blood pressure in patients with essential hypertension and white coat hypertension, Am. J. Chin. Med. 26 (1998) 199–209.

[2] N.D. Kim, S.Y. Kang, V.B. Schini, Ginsenosides evoke endothelium-dependant vascular relaxation in rat aorta, Gen. Pharmacol. 25 (1994) 1071–1077.

[3] N.D. Kim, S.Y. Kang, J.H. Park, V.B. Schini-Kerth, Ginsenoside Rg3 mediates endothelium-dependent relaxation in response to ginsenosides in rat aorta: role of K^+ channels, Eur. J. Pharmacol. 367 (1999) 41–49.

[4] A.G. Herman, S. Moncada, Therapeutic potential of nitric oxide donors in the prevention and treatment of atherosclerosis, Eur. Heart J. 26 (2005) 1945–1955.

[5] H. Kojima, N. Nakatsubo, K. Kikuchi, S. Kawahara, Y. Kirino, H. Nagoshi, Y. Hirata, T. Nagano, Detection and imaging of nitric oxide with novel fluorescent indicators: diaminofluoresceins, Anal. Chem. 70 (1998) 2446–2453.

[6] X. Peng, S. Haldar, S. Deshpande, K. Irani, D.A. Kass, Wall stiffness suppresses Akt/eNOS and cytoprotection in pulse-perfused endothelium, Hypertension 41 (2003) 378–381.

[7] D. Feliers, X. Chen, N. Akis, G.G. Choudhury, M. Madaio, B.S. Kasinath, VEGF regulation of endothelial nitric oxide synthase in glomerular endothelial cells, Kidney Int. 68 (2005) 1648–1659.

[8] I. Fleming, R. Busse, Molecular mechanisms involved in the regulation of the endothelial nitric oxide synthase, Am. J. Physiol. Regul. Integr. Comp. Physiol. 284 (2003) R1–R12.

[9] J. Cho, W. Park, S. Lee, W. Ahn, Y. Lee, Ginsenoside-Rb1 from Panax ginseng C.A. Meyer activates estrogen receptor-alpha and -beta, independent of ligand binding, J. Clin. Endocrinol. Metab. 89 (2004) 3510–3515.

[10] G.B. Phillips, B.H. Pinkernell, T.Y. Jing, The association of hypotesteronemia with coronary artery disease in men, Arterioscler. Thromb. 14 (1994) 701–706.

[11] C.M. Webb, J.G. McNeill, C.S. Hayward, D. De Zeigler, P. Collins, Effects of testosterone on coronary vasomotor regulation in men with coronary heart disease, Circulation 100 (1999) 1690–1696.

[12] F.C. Wu, A. von Eckardstein, Androgens and coronary artery disease, Endocr. Rev. 24 (2003) 183–217.

Exacerbation of Albuminuria and Renal Fibrosis in Subtotal Renal Ablation Model of Adiponectin-Knockout Mice

Koji Ohashi, Hirotsugu Iwatani, Shinji Kihara, Yasuhiko Nakagawa, Noriyuki Komura, Koichi Fujita, Norikazu Maeda, Makoto Nishida, Fumie Katsube, Iichiro Shimomura, Takahito Ito, Tohru Funahashi

Objective—Obesity is recognized increasingly as a major risk factor for kidney disease. We reported previously that plasma adiponectin levels were decreased in obesity, and that adiponectin had defensive properties against type 2 diabetes and hypertension. In this study, we investigated the role of adiponectin for kidney disease in a subtotal nephrectomized mouse model.

Methods and Results—Subtotal (5/6) nephrectomy was performed in adiponectin-knockout (APN-KO) and wild-type (WT) mice. The procedure resulted in significant accumulation of adiponectin in glomeruli and interstitium in the remnant kidney. Urinary albumin excretion, glomerular hypertrophy, and tubulointerstitial fibrosis were significantly worse in APN-KO mice compared with WT mice. Intraglomerular macrophage infiltration and mRNA levels of vascular cell adhesion molecule (VCAM)-1, MCP-1, tumor necrosis factor (TNF)-α, transforming growth factor (TGF)-β1, collagen type I/III, and NADPH oxidase components were significantly increased in KO mice compared with WT mice. Treatment of APN-KO mice with adenovirus-mediated adiponectin resulted in amelioration of albuminuria, glomerular hypertrophy, and tubulointerstitial fibrosis and reduced the elevated levels of VCAM-1, MCP-1, TNF-α, TGF-β1, collagen type I/III, and NADPH oxidase components mRNAs to the same levels as those in WT mice.

Conclusions—Adiponectin accumulates to the injured kidney, and prevents glomerular and tubulointerstitial injury through modulating inflammation and oxidative stress. (***Arterioscler Thromb Vasc Biol.* 2007;27:1910-1917.**)

Key Words: adiponectin ■ obesity ■ subtotal nephrectomy ■ inflammation ■ oxidative stress

Obesity is recognized increasingly as a major risk factor for kidney disease. It has been reported that body mass index (BMI) was associated significantly with increased risk for chronic kidney disease after adjusting for the other confounders.[1]

The adipose tissue produces and secretes many bioactive substances, known as adipocytokines, which directly contribute to obesity-linked metabolic and vascular diseases. Adiponectin is an adipocyte-specific plasma protein that was identified in our laboratories in a human adipose tissue cDNA library.[2] In a series of publications, we reported that physiological concentrations of human recombinant adiponectin suppressed the expression of endothelial adhesion molecules, vascular smooth muscle cell (VSMC) proliferation, macrophage-to-foam cell transformation, and tumor necrosis factor (TNF)-α production by macrophages in vitro.[3-5] We have also shown that adiponectin selectively increased the expression of tissue inhibitor of metalloproteinases, which inhibits extracellular matrix degradation and protects the vascular wall from plaque disruption, in human monocyte-derived macrophages through interleukin (IL)-10 induction, an anti-inflammatory cytokine.[6] Recently, it has been reported that adiponectin exhibited cardioprotective effects after myocardial ischemia/reperfusion through the reduction of oxidative stress.[7] In human studies, we also reported the presence of hypoadiponectinemia in patients with obesity, type 2 diabetes mellitus, and coronary artery disease.[8-10] Interestingly, plasma adiponectin levels are an inverse predictor of cardiovascular outcomes in patients with end-stage renal disease[11] even though plasma adiponectin levels show a negative correlation with GFR through unknown mechanisms.[12]

Experimental subtotal (5/6) renal ablation of mice and rats results in progressive glomerular hypertrophy, podocyte injury, and subsequent fibrosis and proteinuria through adaptive glomerular hyperfiltration,[13,14] oxidative stress,[7] and inflammation.[15] We performed the renal mass reduction by surgical resection of the poles of the kidney rather than by renal artery ligation to prevent the development of severe hypertension, which would be a significant confounding factor in the assessment of the effects of microvascular injury on renal progression.[16] In the present study, we investigated the role of adiponectin against glomerular and tubulointerstitial injury

Original received December 22, 2006; final version accepted June 6, 2007.

From the Departments of Metabolic Medicine (K.O., S.K., Y.N., N.K., K.F., N.M., M.N., F.K., I.S., T.F.) and Nephrology (H.I., T.I.), Graduate School of Medicine, Osaka University, Japan.

K.O. and H.I. contributed equally to this study.

Correspondence to Shinji Kihara, MD, PhD, Department of Metabolic Medicine, Graduate School of Medicine, Osaka University, 2-2 Yamadaoka, Suita, Osaka 565-0871, Japan. E-mail kihara@imed2.med.osaka-u.ac.jp

Arterioscler Thromb Vasc Biol. **is available at http://atvb.ahajournals.org** **DOI: 10.1161/ATVBAHA.107.147645**

using adiponectin-knockout (KO) mice burdened with subtotal renal ablation.

Methods

Animal and Animal Treatment

KO mice were generated as described previously and backcrossed to wild-type (WT) C57BL/6J.[17] Both APN-KO and WT male mice (8- to 10-week-old) were assigned to 2 groups with or without subtotal renal ablation. Subtotal (5/6) nephrectomy was performed by the surgical excision method.[18] All surgical procedures were carried out under anesthesia with intraperitoneal pentobarbital (30 mg/kg body wt; Sigma). The left kidney was exposed through a left paramedian incision and then decapsulated, leaving the adrenal gland intact. The upper and lower poles (two-thirds of the left kidney) were resected, and the remnant kidney was allowed to recover for 1 week. Then the remaining right kidney was removed through a right paramedian incision after ligation of the right renal artery, vein, and ureter. Eight weeks after ablation, KO and WT mice were euthanized for analysis. Tissues were fixed by perfusion of 10% buffered formalin via heart and subsequent immersion in 10% buffered formalin at 4°C for 4 hours. The experimental protocol was approved by the Ethics Review Committee for Animal Experimentation of Osaka University School of Medicine.

Histology and Immunohistochemistry

Four-μm paraffin or optimal cutting temperature (OCT) compound (Sakura) -embedded sections were analyzed immunohistochemically by use of rabbit polyclonal anti-mouse adiponectin antibody (Otsuka Pharmaceutical), goat monoclonal anti-mouse F4/80 antibody (Cedarlane) and goat polyclonal anti-mouse nephrin antibody (Santa Cruz). After incubation with biotin-conjugated secondary antibody, as to adiponectin and nephrin antibody, the specimens were processed by use of the avidin-biotin-peroxidase complex kit (Vector Laboratories). Peroxidase activity was detected with a Liquid DAB Substrate Kit (Zymed Laboratories Inc). As to F4/80, the fluorescent-labeled secondary antibody, Alexa Fluor 488-conjugated guinea pig anti-goat antibody (Molecular Probes), was used. To analyze renal fibrosis, paraffin-embedded sections were stained with periodic acid-Schiff (PAS) method and Masson trichrome method. More than 20 consecutive sections in each mouse were examined, and the mean number of macrophages in the glomeruli was calculated. The number of cells was determined from light microscopic images (Provis AX 80 equipped with an HDTV system and a color-chilled 3 charged coupled device camera; Olympus) using an image analysis system (Macscope version 2.55; Mitani).

Blood Pressure Measurement

Systolic blood pressure (SBP) and heart rate (HR) were measured using the tail cuff technique with an automatic sphygmomanometer (BP98A; Softron) at the tail artery while the animals were restrained. Mice were trained to the tail cuff apparatus at least twice. Ten readings were taken for each measurement, and a mean value was assigned to each individual mouse.

Laboratory Methods

Blood samples were obtained from the retroorbital sinus from these mice before and 4, 6, and 8 weeks after ablation. Spontaneously voided urine was collected between 8 and 11 AM. The blood concentrations of urea nitrogen and creatinine were measured by using appropriate biochemical methods in a commercial laboratory (SRL). Creatinine clearance, in microliters of plasma and urine per minute was calculated by creatinine clearance $CCr=(Cu/Cp)\times V$, where Cu is the concentration of creatinine in urine, Cp is the concentration of creatinine in plasma at the time of a 24-hour urine collection, and V is the urine flow rate in microliters per minute. Urinary albumin excretion was assayed with a murine albumin enzyme-linked immunosorbent assay kit (Exocell). To standardize urinary albumin excretion for GFR, albuminuria was expressed as milligrams of urinary albumin per gram of urinary creatinine. Adiponectin concentrations were determined with ACRP30 ELISA kits (Otsuka Pharmaceutical Co).

Gene Expression Analysis

Total RNA was extracted using RNA-STAT kit (TEL-TEST) according to the protocol supplied by the manufacturer, and 0.5 μg RNA was reverse-transcribed using the ThermoScript RT-PCR system (Invitrogen). Real-time PCR was performed on a LightCycler using the FastStart DNA Master SYBR Green I (Roche Diagnostics) according to the protocol provided by the manufacturer.

We used the primers listed in supplemental materials (available online at http://atvb.ahajournals.org). All results were normalized to 36B4.

Preparation and Delivery of Adenoviral Adiponectin

Adenovirus producing the full-length adiponectin was constructed with Adenovirus Expression Vector Kit (TaKaRa) as described previously.[17] Then, 5×10^8 plaque-forming units of adenovirus-adiponectin (Ad-APN) or adenovirus β-galactosidase (Ad-β gal) was injected intravenously via the tail vein.

Statistical Methods

Data are presented as mean±SEM. Differences between groups were evaluated by the Student t test or analysis of variance (ANOVA) with Fisher PLSD test. A probability value less than 0.05 denoted the presence of a statistically significant difference. All calculations were performed by using a standard statistical package (StatView for Macintosh, version 5.0).

Results

Accumulation of Adiponectin in Glomeruli and Interstitum in Remnant Kidney

Immunohistochemical analysis showed abundant immunostaining for adiponectin in the glomeruli and interstitum of the remnant kidney of WT mice at 8 weeks after subtotal nephrectomy but not in the control glomeruli and interstitum (Figure 1a to 1d). However, real-time PCR showed no detectable level of adiponectin mRNA in the remnant kidney of WT mice (data not shown). These findings indicate accumulation of adiponectin in the glomeruli and interstitum in the injured kidney.

Severe Glomerular Hypertrophy and Tubulointerstitial Fibrosis in Subtotal-Nephrectomized Adiponectin-KO Mice

Subtotal nephrectomy resulted significant rise in urinary excretion of albumin in KO mice but not in WT mice (Table). On the other hand, subtotal nephrectomy did not significantly change levels of blood urea nitrogen, Cr concentrations, creatinine clearance, body weight, SBP, heart rate (HR), or number of glomeruli per section in KO compared with WT mice (Table). Importantly, blood pressure remained within the normal range during our study both in KO and WT mice.

Eight weeks after subtotal nephrectomy, kidney sections of WT mice showed mild glomerular hypertrophy, increased intraglomerular cells mostly in the mesangial area, and tubulointerstitial fibrosis (compare Figure 2a and 2b with 2e and 2f). These changes were more severe in adiponectin-KO mice (compare Figure 2c and 2d with 2g and 2h).

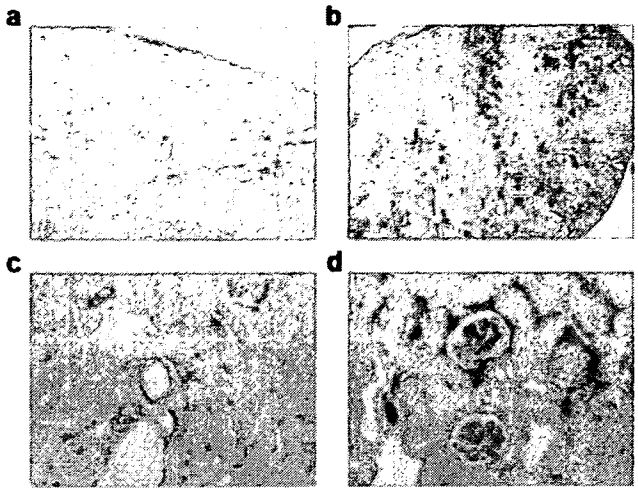

Figure 1. Representative results of immunohistochemical analyses for adiponectin in non-operated WT (a and c) and WT mice after subtotal nephrectomy (b and d). Control nonoperated mice showed limited glomerular and tubulointerstitial staining for adiponectin (a and c), whereas glomerular and tubulointerstitial immunostaining for adiponectin was augmented after subtotal nephrectomy (b and d). Magnification, ×40 (a and b), ×200 (c and d).

To analyze these changes quantitatively, the glomerular cross-sectional area and number of intraglomerular cells in every specimen were measured (Figure 2i through 2k). Without subtotal nephrectomy, the average cross-sectional area and number of intraglomerular cells of control KO mice were similar to those of control WT mice [cross-sectional area (mm^2): $2.55\pm0.01\times10^{-3}$ for KO mice (n=6), $2.52\pm0.11\times10^{-3}$ for WT mice (n=6); intraglomerular cell number (cells/glomerulus): 23.9±0.8 for KO mice, 23.8±1.2 for WT mice; Figure 2i and 2j)]. On the other hand, subtotal nephrectomy resulted in increases in glomerular cross-sectional area and number of intraglomerular cells of both WT (n=6) and KO (n=8) mice at 8 weeks (cross-sectional area: $2.72\pm0.11\times10^{-3}$ and $3.13\pm0.11\times10^{-3}$ mm^2, respectively, intraglomerular cell number: 34.3±1.0 and 38.3±1.4/section, respectively, Figure 2i and 2j). These increases were more significant in KO mice than in WT mice ($P<0.05$, for both, Figure 2i and 2j). Furthermore, subtotal nephrectomy resulted in increase area of tubulointerstitial fibrosis in both WT and KO mice (Figure 2k), which was also significantly more severe in KO mice (7.6±1.1%) than in WT mice (4.7±0.3%; $P<0.05$). Nephrin immunostaining tended to reduce in the remnant kidneys of both WT and KO mice by subtotal renal ablation (supplemental Figure I-a, I-b, I-c, and I-d). To quantify the expression of nephrin, quantative real-time PCR was performed in the control and remnant kidney. Subtotal nephrectomy resulted in significant reduction of nephrin mRNA levels in the remnant kidney in KO mice than in WT mice (supplemental Figure I-e). Adiponectin deficiency had no effect on nephrin mRNA levels without renal ablation.

Inflammatory Response in Adiponectin KO Mice and WT Mice

Next, we investigated glomerular macrophage infiltration, which is regarded as a key event in glomerular injury that leads to renal fibrosis and proteinuria. Immunohistochemical analysis revealed increased number of glomerular infiltration of F4/80-positive macrophages in KO mice after renal ablation (Figure 3a). The gene expressions of F4/80 and CD68, which were specifically expressed in macrophages and macrophage-related cells, were significantly increased in KO mice after subtotal nephrectomy (supplemental Figure II-a). To determine the mechanism of severe glomerular and tubulointerstitial damage in KO mice, we examined the mRNA levels of proteins associated with macrophage infiltration, glomerular and tubulointerstitial fibrosis, oxidative stress, and chronic hypoxia. Subtotal nephrectomy resulted in significant overexpression of VCAM-1, MCP-1, TNF-α, TGF-β1, collagen I, and collagen III mRNA levels in the remnant kidney in KO mice than in WT mice (Figure 3b and 3c). The mRNA levels of NADPH oxidase components, $gp91^{phox}$, $p47^{phox}$, and $p67^{phox}$, were increased in the remnant kidney in KO mice than in WT mice (Figure 3d). On the other hand, there were no significant differences in the mRNA expression levels of catalase and Cu,Zn-SOD, as antioxidant enzymes, between KO and WT mice, although subtotal nephrectomy significantly reduced antioxidant enzyme mRNA levels both of KO and WT mice (supplemental Figure II-b). There were no significant differences in the mRNA levels of VEGF-A, as

Characteristics of Adiponectin Knockout (KO) and Wild-Type (WT) Mice

	Control		Subtotal Nephrectomy	
Parameters	WT (n=6)	KO (n=6)	WT (n=6)	KO (n=8)
Body Weight, g	32.7±1.2	31.6±1.2	27.6±0.5	27.1±0.7
Systolic blood pressure, mm Hg	103.0±1.7	103.0±1.3	103.2±3.0	102.0±0.8
Heart rate, beat/min	681.2±12.9	675.8±20.2	705.0±24.1	717.4±12.3
No. of glomeruli/section	184.6±10.9	176.5±7.9	73.5±5.7	70.3±2.1
Blood urea nitrogen, mg/dl	29.3±3.6	28.0±1.8	70.0±4.0	72.5±4.5
Serum creatinine, mg/dl	0.11±0.02	0.09±0.01	0.25±0.01	0.25±0.02
Creatinine Clearance, μl/min	208.1±22.0	174.7±35.8	113.0±14.9	101.5±10.9
Serum adiponectin, μg/ml	19.0±1.4	ND	32.2±3.9	ND
Urinary albumin, mg/g Cr	35.2±21.5	27.1±6.1	52.2±11.4	99.4±14.8*

Data are mean±SEM. $P<0.05$ compared with WT after subtotal nephrectomy. ND indicates not detectable.

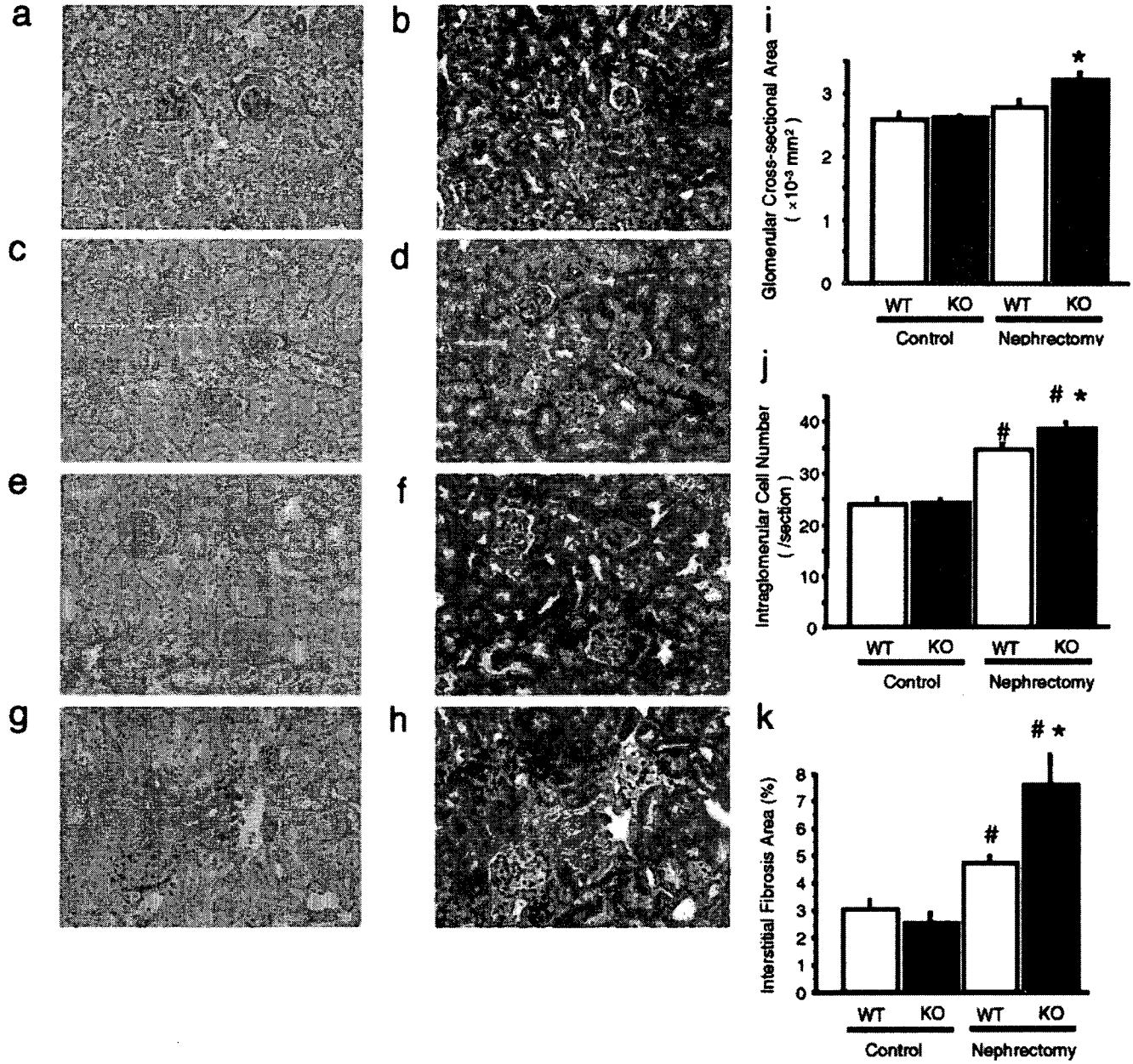

Figure 2. a through h, Histology of the kidneys of nonoperated WT (a and b), nonoperated KO (c and d), and WT (e and f) and KO (g and h) mice after subtotal nephrectomy. Representative periodic acid-Schiff (PAS)-stained sections (a, c, e, and g) and Masson trichrome stained sections (b, d, f, and h). Note the lack of differences in the glomeruli and tubules between nonoperated WT and KO mice (a and c, b and d). Eight weeks after subtotal nephrectomy, glomerular hypertrophy and tubulointerstitial fibrosis were only modestly increased in WT mice (e and f) but remarkably increased in KO mice (g and h). Mean values of area of glomerular cross-section (i), number of intraglomerular cells (j), and area of interstitial fibrosis (k) were quantitatively analyzed for WT and KO mice with or without subtotal nephrectomy. Magnification, ×200. #$P<0.05$ for control WT mice. *$P<0.05$ for renal-ablated WT mice.

the downstream of hypoxia inductive factor-1α (supplemental Figure II-b).

Adiponectin Supplementation Ameliorates Albuminuria, Glomerular Hypertrophy, and Tubulointerstitial Fibrosis in Subtotal Nephrectomized-KO Mice

To determine the effect of exogenous adiponectin replenishment, KO and WT mice were treated with Ad-APN or Ad-β gal. Four weeks after subtotal nephrectomy, Ad-APN or Ad-β gal was injected intravenously via the tail vein. On day 14 postinjection, plasma adiponectin levels were 65.1±22.9 μg/mL in KO mice treated with Ad-APN (KO/Ad-APN, n=9), not detectable in KO mice treated with Ad- β gal (KO/Ad-β gal, n=9), 59.7±9.2 μg/mL in WT/Ad-APN (n=10), and 19.1±2.0 μg/mL in WT/Ad-β gal (n=9). Immunohistochemical analysis at 4 weeks after Ad-APN injection showed adiponectin accumulation in the glomeruli and interstitum of the remnant kidneys of KO mice (Figure 4a). Such immunohistochemical improvement was coupled with significant decrease in urinary albumin excretion/Cr (mg/g Cr) in KO/Ad-APN compared with KO/Ad-β gal after